

1 **PfaSTer: A ML-powered serotype caller for *Streptococcus pneumoniae* genomes**

2 Jonathan T. Lee^{a#}, Xingpeng Li^b, Craig Hyde^b, Paul A. Liberator^a, Li Hao^a

3

4 ^aVaccine Research & Development, Pfizer Inc. 401 N. Middletown Rd, Pearl River, NY 10965, USA

5 ^bEarly Clinical Development, Pfizer Inc. 1 Portland St, Cambridge, MA 02139, USA

6 [#]Corresponding author: Jonathan T. Lee, Jonathan.Lee@pfizer.com

7

8 **Abstract**

9 *Streptococcus pneumoniae* (pneumococcus) is a leading cause of morbidity and mortality worldwide.
10 Although multi-valent pneumococcal vaccines have curbed the incidence of disease, their introduction
11 has resulted in shifted serotype distributions that must be monitored. Whole genome sequence (WGS)
12 data provides a powerful surveillance tool for tracking isolate serotypes, which can be determined from
13 nucleotide sequence of the capsular polysaccharide biosynthetic operon (*cps*). Although software exists to
14 predict serotypes from WGS data, their use is constrained by the requirement of high-coverage Next
15 Generation Sequencing (NGS) reads. This can present a challenge in so far as accessibility and data
16 sharing. Here we present PfaSTer, a method to identify 65 prevalent serotypes from individual *S.*
17 *pneumoniae* genome sequences rather than primary NGS data. PfaSTer combines dimensionality
18 reduction from k-mer analysis with machine learning, allowing for rapid serotype prediction without the
19 need for coverage-based assessments. We then demonstrate the robustness of this method, returning
20 >97% concordance when compared to biochemical results and other *in-silico* serotypers. PfaSTer is open
21 source and available at: <https://github.com/pfizer-opensource/pfaster>.

22
23

24 **Introduction**

25 *Streptococcus pneumoniae* (pneumococcus) presents a major concern to public health, being a common
26 cause of lower respiratory tract infections and pneumonia [1, 2]. Pneumococcal disease is a particular
27 threat to the elderly, largely due to a high mortality risk when contracting pneumonia [1, 3].
28 Pneumococcal conjugate vaccines (PCVs) can be used to prevent disease [4, 5] by affording protection
29 against common circulating serotypes. In *S. pneumoniae*, serotype is defined by the structure of a capsular
30 polysaccharide and the genes that direct biosynthesis of the polysaccharide encoded at the capsular
31 polysaccharide synthesis (*cps*) operon [6]. To date, over 95 pneumococcal serotypes carrying unique *cps*
32 sequences have been identified [7], with a fraction of these found to be prevalent in global populations

33 [7]. As the capsular polysaccharide serves as the target of PCVs [4], surveillance of emerging strains
34 through serotyping is important for monitoring efficacy against circulating strains and the development of
35 new multi-valent vaccines [8].

36 Traditionally, pneumococcal serotyping is performed using serotype-specific monoclonal antibody
37 reagents, either through the Quellung reaction or latex agglutination [9]. While held in high regard, such
38 methods are expensive and laborious [9, 10]. Antibody tests are also often unable to differentiate closely
39 related serotypes [9, 11], and visual assessment of agglutination results are susceptible to subjective
40 interpretation. Furthermore, the need for cell cultures presents a physical barrier for replicating results
41 between research groups. As an alternative, automated pipelines for predicting serotypes from Next
42 Generation Sequencing (NGS) data have been developed. Since 2016, PneumoCaT, SeroBA, and more
43 recently SeroCall, have been utilized to effectively identify serotypes *in-silico* [10, 12, 13]. While their
44 underlying algorithms differ, these methods all utilize the same input: raw NGS data from the *cps* locus
45 and a reference *cps* database for different serotypes. By leveraging an abundance of NGS reads, these
46 applications provide robust predictions of the *cps* sequence and therefore the *in-silico* serotype.

47 While a powerful resource, high-coverage NGS data can be unwieldy and computationally intensive to
48 work with. Furthermore, such data is not always readily available to researchers. For instance, the
49 PubMLST [14] microbial database contains, to date, over 30,000 pneumococcal genomes from
50 submissions around the globe. Many of these assembled genomes lack accompanying NGS data sources
51 and would be incompatible with the previously described serotyping tools.

52 We developed the pneumococcal FASTA serotyper (PfaSTer) to address the need for *in-silico* serotyping
53 when constrained to working with assembled or aligned genome sequences. PfaSTer identifies k-mers at
54 the *cps* locus associated with each serotype, which are utilized in machine learning for prediction (Fig 1).
55 Using a validated dataset of >2,000 pneumococcal isolates, we show that PfaSTer is both a fast and
56 highly accurate serotype caller, with predictions comparable to both serological results and other
57 computational methods.

58

59 **Materials and Methods**

60 *Data sources*

61 Training data for PfaSTer was obtained from the Sanger Institute Pathogenwatch platform
62 (pathogen.watch) in the form of de-novo assembled genomes for isolates spanning 65 different serotypes
63 (Table S1). For validation, sequences were obtained from the NCBI sequence read archive. Accessions
64 for these data can be found in (Table S2).

65

66 *Mash sketch creation*

67 Reference *cps* sequences (previously published and utilized by PneumoCAT [12] and seroBA [10]) were
68 used to develop a MinHash sketch [15] of 65 serotypes. A sliding window (k-mer) of 70 nucleotides was
69 used to scan each *cps* sequence, with each k-mer converted to a 128 bit integer using MurmurHash3
70 (v3.0.0). To account for bidirectionality, both the forward and reverse complemented k-mer were
71 considered and the lexicographically smaller sequence used for hashing. The k-mers corresponding to the
72 1,000 smallest integer values for each serotype were saved to the sketch.

73

74 *Model training and probability thresholding*

75 A Mash screen [16] was performed for 4,019 pneumococcal genomes using the previously described
76 sketch. Each hash of 70 base pair k-mers in a sliding window across the genome sequence was compared
77 to those in the reference sketch, and matching k-mers recorded. The total number of k-mers matched for
78 each serotype were then saved and used as features to train a Random Forest classifier using the R
79 tidymodels package (v0.1.2). To account for class imbalance due to differences in serotype prevalence,
80 overrepresented serotypes were down sampled to no more than 200 cases for training. Initial model

81 performance was measured using a grid search and the average accuracy across 2000 internal cross-
82 validations. The model was then ported to python using the sklearn package (v1.1.1). Hyperparameter
83 tuning was performed using a grid-search, with optimal parameters found to be 300 estimators, 10
84 features per estimator, and 4 samples to split branches. Model performance was re-calculated and reported
85 using the average accuracy across 200 internal cross-validations.

86 To limit errant predictions, the model-computed probability of both correct and incorrect predictions was
87 recorded for each serotype based on the training dataset in cross-validation. For each sample, the serotype
88 with the highest prediction probability was saved and noted as correct or incorrect classification compared
89 to their labeled serotype. The probability distributions of correct and incorrect classifications were used to
90 fit a generalized linear model with a binomial distribution for each of 17 serotypes. For cases where the
91 two distributions did not overlap, a minimum probability threshold was determined as $(\ln(p/(1-p)) - b_0)/b_1$,
92 where b_0 is the fitted intercept, b_1 the slope, and $p = 0.05$. For cases where the distributions did overlap,
93 the minimum threshold was calculated using the upper limit of the one-side 95% confidence interval of
94 the incorrect classification distribution.

95

96 *Feature alignment for closely related serotypes*

97 Reference sequences for *wciZ* (serotype 15B), *wciX* (serotype 18C), and *wciG* (serotype 35B) were
98 obtained from annotated genomes at NCBI (accessions CR931664, CR931673, and KX021817,
99 respectively). BLASTN [17] was used to obtain the sequence of the corresponding gene for each
100 serotype, and the resulting reading frame was assessed for presence of a premature stop codon.

101

102 *Validation with an external dataset*

103 A collection of short-read sequencing data for 2,065 UK isolates originally from Public Health England
104 was used for validation. Reads were de-novo assembled to genome sequences using SPAdes (v3.14.0, -
105 isolate mode) [18] and serotypes predicted using PfaSTer. Isolates that were previously labeled through
106 latex agglutination [10] to be non-typeable, or serotypes not supported by PfaSTer, were excluded from
107 calculations. This resulted in validation against 2,026 samples (Table S2). PfaSTer predicted serotypes
108 were compared to latex agglutination results as well as calls made by both PneumoCaT and SeroBA –
109 previously reported in [10] (Note S1).

110

111 **Results**

112 We sought to develop a method for predicting pneumococcal serotypes relying only on minimal data in
113 the form of consensus genome sequences. To this end, we first applied the MinHash (Mash) algorithm, a
114 dimensionality-reduction technique that can effectively compress up to entire genome sequences to a
115 small collection (or *sketch*) of several thousand sub-sequences (k-mers) [15]. As the capsular
116 polysaccharide is encoded at the *cps* operon, we started by performing a Mash Screen [16] comparing
117 >4,000 pneumococcal genomes against a k-mer sketch of each serotype's *cps* locus. The number of
118 matched k-mers to each serotype was then used as features to train a Random Forest classifier. This
119 method predicts the pneumococcal serotype based on the collective voting of hundreds of decision tree
120 estimators, each trained on a bootstrapped set of the >4,000 training samples.

121 Through internal cross-validation, we found the resulting model yielded a median accuracy of 97.8% in
122 our training data. To account for misclassification from low-confidence predictions, we recorded the
123 prediction probabilities returned by the Random Forest model during cross-validation and calculated the
124 probability distributions of correct and incorrect serotype calls (Fig S1). We then set thresholds based on
125 the 95% confidence intervals, flagging serotype predictions below these values as low-confidence.
126 Following this addition, most remaining misclassifications resulted from closely related serotypes, which

127 could not be distinguished using the Mash screen results due to a high density of shared k-mers (Fig S2).
128 In particular, the serotype pairs 15B/C, 18B/C, 24B/F, and 35B/D had a higher rate of incorrect serotype
129 calls compared to other types during cross-validation (Table S3). While the genetic cause of the 24B and
130 24F capsular polysaccharides has previously been hypothesized and studied [6, 19], the exact mechanism
131 underlying their differing polysaccharide structures is still unclear. As we cannot reliably distinguish
132 serotype 24B from 24F at this time, PfaSTer reports Serogroup 24 when either of these types is predicted
133 by the model. In contrast, modifications that inactivate genes that code for O-acetyltransferases (*wciZ* for
134 15B/C, *wciX* for 18B/C, and *wxiG* for 35B/D) [20-22] impact polysaccharide structure and serotype
135 designations. These modifications can include in/dels as well as SNVs leading to frame shifts and/or
136 premature stop codons. Unfortunately, subtle and heterogeneous modifications that inactivate a step in
137 polysaccharide biosynthesis and therefore polysaccharide structure are generally not detectable with the
138 Mash screen technique.

139 To overcome this challenge in classifying 15B/C, 18B/C, and 35B/D isolates, we added a local alignment
140 stage when one of these serotypes is predicted by our model. This step searches the corresponding
141 acetyltransferase for premature termination that would inactivate the protein. By applying this check, we
142 were able to successfully assign each isolate to the correct serotype.

143 As final validation, we applied the PfaSTer prediction pipeline to 2,026 isolates previously evaluated
144 using the *in-silico* serotyping tools PneumoCaT [12] and SeroBA [10], both of which utilize NGS read
145 data as inputs. Compared to results from latex agglutination, PfaSTer showed 97.09% concordance in its
146 serotype predictions (Fig 2, Table S2). This is similar to the ~98% concordance previously reported by
147 Epping et al using PneumoCat and SeroBA [10]. Furthermore, serotype calling by PfaSTer was in high
148 concordance with the other computational methods, returning the same serotype as PneumoCaT in
149 97.97% of cases and SeroBA in 98.47% of cases (Fig 2, Table S2). PfaSTer also demonstrated an
150 extremely rapid runtime during this benchmarking, with all 2,026 samples completed in under 2 hours on
151 a 36 cpu Amazon EC2 c4 instance running 8 parallel processes.

152 Among the isolates used for comparison, 17 were not typed by PfaSTer due to prediction probabilities
153 falling below our computed thresholds. For cases where PfaSTer predicted a serotype with high
154 confidence, most disagreement with other typing methods occurred with 15C and 35D designations
155 (Table S2). There were 19 instances where results from latex agglutination, PneumoCaT, and SeroBA
156 differed from not only PfaSTer, but also one-another when calling the serotype as 15B or 15C. PfaSTer
157 also identified six isolates as serotype 35D, which were identified as 35B by PneumoCaT and latex
158 agglutination. As an additional validation, we saved the *wciG* alignments for the six 35D predictions, and
159 the *wciZ* alignments for five randomly selected 15C predictions that differed from latex agglutination. We
160 then reviewed the resulting protein sequences for truncation. In all cases, a premature stop was indeed
161 observed in the corresponding O-acetyltransferase (Fig S3). These isolates are therefore expected to
162 express 15C or 35D capsular polysaccharide, as predicted by PfaSTer.

163

164 **Discussion**

165 We have developed an efficient tool for rapid *in-silico* serotyping of *S. pneumoniae* from assembled
166 genome sequences. This method uses a single-pass k-mer screen and a machine learning model to predict
167 the *S. pneumoniae* serotype without needing to access raw NGS data. While a targeted alignment step is
168 included to resolve a small subset of serotype-specific features (a limitation shared among serotyping
169 pipelines [10, 12]), high density read data is not needed, in contrast to other published tools.

170 A major challenge in developing PfaSTer was establishing confidence in the serotype predictions when
171 constrained to a single genome sequence. While other *in-silico* algorithms designed to assign serotype
172 utilize per-base or per-k-mer coverage to generate confidence, this information is unavailable when
173 working with a single consensus genome. Although the Mash screen results estimate sequence similarity
174 to each serotype, they do not provide any statistical power on their own. This challenge was addressed at
175 the machine learning step by leveraging the innate properties of the Random Forest model. As the model

176 consists of an ensemble of decision trees, prediction probability can be estimated as the proportion of
177 trees agreeing on the serotype [23]. Using these values, thresholds were established to flag low-
178 confidence serotype predictions. These probability estimates are also provided to users of PfaSTer to
179 support their own decision making.

180 Of the >2,000 isolates used to validate PfaSTer performance, a small fraction exhibited discordance with
181 other serotyping methods. This included 17 samples that did not return a serotype due to low-confidence
182 prediction. Of note, 5 of these isolates were unable to be typed with other *in-silico* pipelines or were
183 reported as a mixture of serotypes (Table S2). This suggests that predictions computed at low probability
184 may be caused in-part by low quality sequencing data.

185 Discordance was also noted in instances when PfaSTer identified mutations that predict the derived
186 serotypes 15C and 35D. In those samples latex agglutination called the serotype as 15B or 35B,
187 respectively. Notably, each of samples with a lack of 15B/15C concordance mapped to mutations in the
188 same region of *wciZ* at a TA-tandem repeat that has been shown to slip and cause indels during
189 replication (Fig S4) [24, 25]. As repeated frameshifts can convert the serotype between 15B (complete
190 *wciZ* gene and intact O-acetyltransferase open reading frame) and 15C, the serotype can switch over time.
191 [12, 24]. Additionally, as antibodies against 15B have been shown to cross-react with 15C polysaccharide
192 [20, 25], mislabeling could occur when typing with antisera. In contrast to 15C, 35D-causing mutations
193 were more widely distributed across *wciG*, causing premature termination at different positions along the
194 protein coding sequence (Fig S3B). PneumoCaT does not appear to support the identification of serotype
195 35D, only able to provide a 35B assignment for the samples included in this study. Like the output from
196 PfaSTer, the SeroBA tool also recognized this subset of isolates as serotype 35D.

197 Although both fast and powerful, serotype assignment using PfaSTer has certain restrictions. As PfaSTer
198 relies on a supervised learning model for prediction, enough cases must be available for training. While
199 over 95 pneumococcal serotypes have been recorded [26], certain serotypes are more prevalent than
200 others throughout the world. As a result, PfaSTer prediction is limited to 65 types due to a shortage of

201 available genomes for rare serotypes. From recent studies, commonly collected serotypes shared across
202 the US, Europe, and Asia include 1, 3, 6A, 6B, 14, 18C, 19F, and 23F, with other serotypes identified at
203 lower frequency [27-31]. Unsurprisingly, these prevalent serotypes are all included in the pneumococcal
204 conjugate vaccine (PCV) formulations of PCV13 [32] and PCV20 [8]. To support continual estimation of
205 vaccine coverage, the commonly circulating serotypes in these PCV formulations are all supported by
206 PfaSTer. As the serotype landscape changes over time, and genomes of new isolates are made available,
207 the number of serotypes predicted by PfaSTer may rise.

208 By relying on an assembled genome, PfaSTer also has reduced functionality for mixed samples compared
209 to some alignment-based serotype tools. For instance, the SeroCall [13] tool can identify both major and
210 minor serotypes in mixed sequencing data by aligning sequencing reads to multiple references. While
211 PfaSTer does not support prediction for assembled metagenomes, the presence of each serotype can
212 potentially be inferred from the density of k-mers present in the Mash screen step [16]. Future
213 developments on PfaSTer could address this feature more directly.

214 As global monitoring and sequencing of *S. pneumoniae* continues, PfaSTer provides a means to leverage
215 portable, but previously underutilized, genome sequences for data sharing and serotype tracking. Such
216 surveillance efforts could have important impact on understanding the spread of *S. pneumoniae* and
217 influence future vaccine design for combatting pneumococcal disease. Finally, this method may have
218 applications suitable for typing of other microbial species beyond *S. pneumoniae*.

219

220 **Data Summary**

221 PfaSTer is open source and available for Linux on Github under Apache License v2.0 at
222 <https://github.com/pfizer-opensource/pfaster>

223 Accession numbers for sequencing data are listed in the supplementary material.

224

225 **Acknowledgements**

226 The authors would like to thank Charles Tan for his assistance in statistical modeling, and Scott Perrin for
227 digital help in deploying PfaSTer. We also thank Varun Raghuraman for his efforts testing the installation
228 and running of PfaSTer, Zhenghui Li and Andy Weiss for critical reading of the manuscript, and Christina
229 D'Arco for scientific writing assistance.

230 **Author Contributions**

231 All authors met ICMJE criteria for authorship and participated in the study design and conceptualization
232 (JL, XL, CH, PL, LH), methods development and data interpretation (JL, XL), writing – original draft
233 (JL, XL, LH), and manuscript preparation (JL, XL, CH, PL, LH).

234

235 **Funding Information**

236 This research received no specific grant from any funding agency in the public, commercial, or not-for-
237 profit sectors. This study was solely sponsored by Pfizer, Inc.

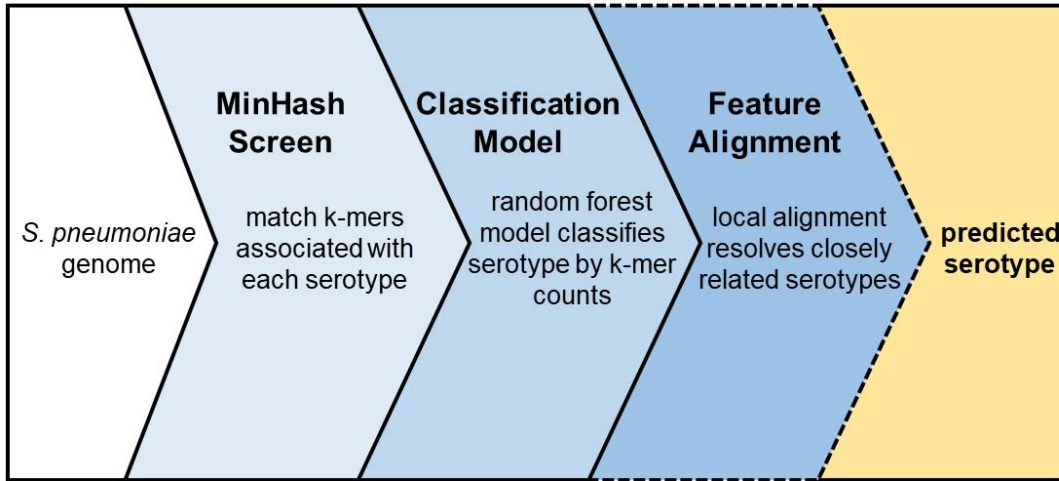
238

239 **Conflicts of Interest**

240 All authors are employees of Pfizer Inc. and some authors are Pfizer stock owners.

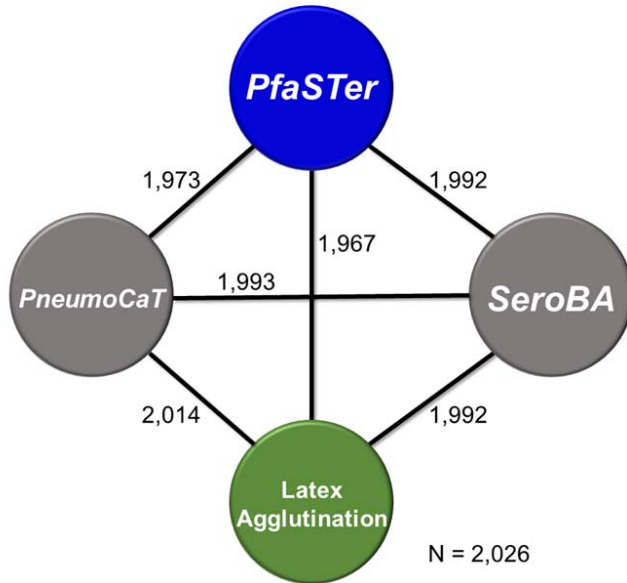
241

242 **Figures and Tables**



243

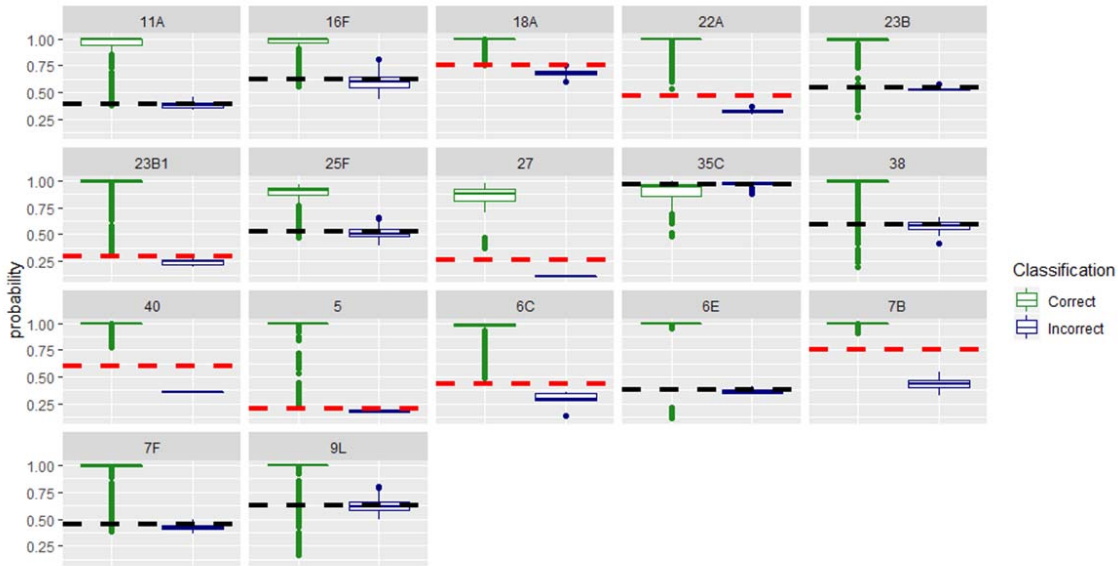
244 **Fig 1: PfaSTer workflow.** PfaSTer takes an aligned or assembled *S. pneumoniae* genome sequence
245 (FASTA format) as an input. A MinHash screen for k-mers associated with each reference serotype is
246 first performed. The number of k-mers matched to each reference is then passed to a Random Forest
247 classifier to assign a predicted serotype. In cases where the model is unable to discern closely-related
248 types, alignment is performed to identify serotype-defining features.



249

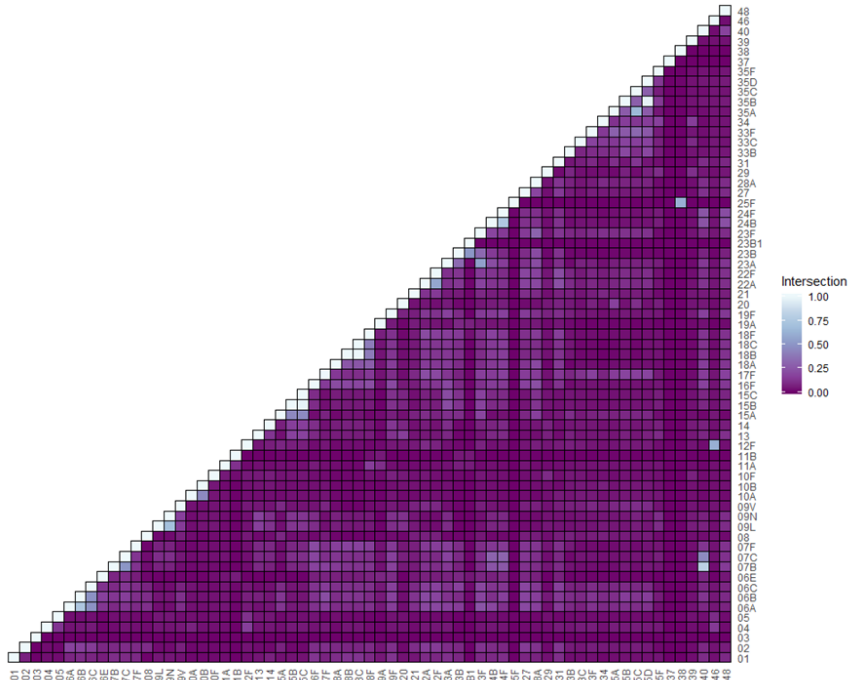
250 **Fig 2: Concordance between serotyping methods for a validated dataset.** Number of isolates (out of
251 2,026) returning the same serotype when tested using PfaSTer, latex agglutination, and two other *in-silico*
252 serotyping tools

253 .



254

255 **Fig S1: Probability thresholds for 17 serotypes.** Model-computed probability distributions for correct
256 and incorrect predictions from cross-validation are shown for 17 serotypes that returned incorrect
257 predictions during model development. Red lines indicate the calculated probability thresholds when
258 distributions do not overlap, and black lines when tails of the distributions do overlap. Predictions made
259 at a probability below these set values are flagged as low-confidence. Calculations for modeling the
260 probability distributions and threshold determination are described in the Materials and Methods.



261

262 **Fig S2: MinHash overlap across serotypes.** Fraction of k-mers shared between each pair of 65 serotype

263 MinHash sketches. Proportions correspond to overlap ranging from 0 to 1,000 k-mers.

264

265



266

267 **Fig S3: Amino acid sequences of O-acetyltransferases in 15C and 35D isolates predicted by**
268 **PfaSTer.** A) Alignment of a serotype 15B WciZ sequence to five isolates predicted as serotype 15C by
269 PfaSTer. Two variants of WciZ were observed across five isolates, both containing a premature stop prior
270 to residue 150. B) Alignment of a serotype 35B WciG sequence to six isolates predicted to be serotype
271 35D by PfaSTer. Three sequences terminate prematurely prior to residue 140, and three terminate further
272 downstream prior to residue 320.

wciZ (15B) 401 TATTTGCTAT ATT~~ATATATA~~ ~~TATATATATC~~ TTTATTTTC 440
ERR1439297 TATTTGCTAT ATTATATATA TATATAT~~TC~~ TTTATTTTC
ERR1436407 TATTTGCTAT ATTATATATA TATATAT~~TC~~ TTTATTTTC
ERR1439409 TATTTGCTAT ATTATATATA TATATAT~~TC~~ TTTATTTTC
ERR1439231 TATTTGCTAT ATTATATATA T~~TC~~ TTTATTTTC
ERR1439342 TATTTGCTAT ATTATATATA T~~TC~~ TTTATTTTC

273

274 **Fig S4: Frameshift mutations at a tandem repeat region of *wciZ* in serotype 15C.** Isolates predicted
275 to be serotype 15C by PfaSTer carry multiple nucleotide deletions (red) in an AT-rich tandem repeat
276 (yellow) relative to a 15B reference sequence. Previous work has shown that the resulting frameshift
277 inactivates the WciZ protein and causes formation of the 15C capsular polysaccharide.

278

279 **Table S1: Isolate names (pathogen.watch) and serotypes for samples used in PfaSTer training.**

280 **Table S2: ENA accessions and serotype caller results for isolates used in external validation.**

281 **Table S3: Fraction of incorrect prediction for each serotype class during cross validation.**

282

283

284 **References**

- 285 1. Blasi, F., et al., *Understanding the burden of pneumococcal disease in adults*. Clin Microbiol
286 Infect, 2012. **18 Suppl 5**: p. 7-14.
- 287 2. Collaborators, G.B.D.L.R.I., *Estimates of the global, regional, and national morbidity, mortality,
288 and aetiologies of lower respiratory infections in 195 countries, 1990-2016: a systematic analysis
289 for the Global Burden of Disease Study 2016*. Lancet Infect Dis, 2018. **18**(11): p. 1191-1210.
- 290 3. Drijkoningen, J.J. and G.G. Rohde, *Pneumococcal infection in adults: burden of disease*. Clin
291 Microbiol Infect, 2014. **20 Suppl 5**: p. 45-51.
- 292 4. Harboe, Z.B., et al., *Impact of 13-valent pneumococcal conjugate vaccination in invasive
293 pneumococcal disease incidence and mortality*. Clin Infect Dis, 2014. **59**(8): p. 1066-73.
- 294 5. McLaughlin, J.M., et al., *Effectiveness of 13-Valent Pneumococcal Conjugate Vaccine Against
295 Hospitalization for Community-Acquired Pneumonia in Older US Adults: A Test-Negative Design*.
296 Clin Infect Dis, 2018. **67**(10): p. 1498-1506.
- 297 6. Mavroidi, A., et al., *Genetic relatedness of the *Streptococcus pneumoniae* capsular biosynthetic
298 loci*. J Bacteriol, 2007. **189**(21): p. 7841-55.
- 299 7. Hausdorff, W.P. and W.P. Hanage, *Interim results of an ecological experiment - Conjugate
300 vaccination against the pneumococcus and serotype replacement*. Hum Vaccin Immunother,
301 2016. **12**(2): p. 358-74.
- 302 8. Essink, B., et al., *Pivotal Phase 3 Randomized Clinical Trial of the Safety, Tolerability, and
303 Immunogenicity of 20-Valent Pneumococcal Conjugate Vaccine in Adults Aged >/=18 Years*. Clin
304 Infect Dis, 2022. **75**(3): p. 390-398.
- 305 9. Jauneikaite, E., et al., *Current methods for capsular typing of *Streptococcus pneumoniae**. J
306 Microbiol Methods, 2015. **113**: p. 41-9.

307 10. Epping, L., et al., *SeroBA: rapid high-throughput serotyping of Streptococcus pneumoniae from*
308 *whole genome sequence data*. *Microb Genom*, 2018. **4**(7).

309 11. Porter, B.D., B.D. Ortika, and C. Satzke, *Capsular Serotyping of Streptococcus pneumoniae by*
310 *latex agglutination*. *J Vis Exp*, 2014(91): p. 51747.

311 12. Kapatai, G., et al., *Whole genome sequencing of Streptococcus pneumoniae: development,*
312 *evaluation and verification of targets for serogroup and serotype prediction using an automated*
313 *pipeline*. *PeerJ*, 2016. **4**: p. e2477.

314 13. Knight, J.R., et al., *Determining the serotype composition of mixed samples of pneumococcus*
315 *using whole-genome sequencing*. *Microb Genom*, 2021. **7**(1).

316 14. Jolley, K.A., J.E. Bray, and M.C.J. Maiden, *Open-access bacterial population genomics: BIGSdb*
317 *software, the PubMLST.org website and their applications*. *Wellcome Open Res*, 2018. **3**: p. 124.

318 15. Ondov, B.D., et al., *Mash: fast genome and metagenome distance estimation using MinHash*.
319 *Genome Biol*, 2016. **17**(1): p. 132.

320 16. Ondov, B.D., et al., *Mash Screen: high-throughput sequence containment estimation for genome*
321 *discovery*. *Genome Biol*, 2019. **20**(1): p. 232.

322 17. McGinnis, S. and T.L. Madden, *BLAST: at the core of a powerful and diverse set of sequence*
323 *analysis tools*. *Nucleic Acids Res*, 2004. **32**(Web Server issue): p. W20-5.

324 18. Bankevich, A., et al., *SPAdes: a new genome assembly algorithm and its applications to single-*
325 *cell sequencing*. *J Comput Biol*, 2012. **19**(5): p. 455-77.

326 19. Ganaie, F., et al., *Structural, Genetic, and Serological Elucidation of Streptococcus pneumoniae*
327 *Serogroup 24 Serotypes: Discovery of a New Serotype, 24C, with a Variable Capsule Structure*. *J*
328 *Clin Microbiol*, 2021. **59**(7): p. e0054021.

329 20. Spencer, B.L., et al., *The Pneumococcal Serotype 15C Capsule Is Partially O-Acetylated and*
330 *Allows for Limited Evasion of 23-Valent Pneumococcal Polysaccharide Vaccine-Elicited Anti-*
331 *Serotype 15B Antibodies*. *Clin Vaccine Immunol*, 2017. **24**(8).

332 21. McEllistrem, M.C., *Genetic diversity of the pneumococcal capsule: implications for molecular-*
333 *based serotyping*. *Future Microbiol*, 2009. **4**(7): p. 857-65.

334 22. Lo, S.W., et al., *Global Distribution of Invasive Serotype 35D Streptococcus pneumoniae Isolates*
335 *following Introduction of 13-Valent Pneumococcal Conjugate Vaccine*. *J Clin Microbiol*, 2018.
336 **56**(7).

337 23. Malley, J.D., et al., *Probability machines: consistent probability estimation using nonparametric*
338 *learning machines*. *Methods Inf Med*, 2012. **51**(1): p. 74-81.

339 24. van Selm, S., et al., *Genetic basis for the structural difference between Streptococcus*
340 *pneumoniae serotype 15B and 15C capsular polysaccharides*. *Infect Immun*, 2003. **71**(11): p.
341 6192-8.

342 25. Hao, L., et al., *Streptococcus pneumoniae serotype 15B polysaccharide conjugate elicits a cross-*
343 *functional immune response against serotype 15C but not 15A*. *Vaccine*, 2022. **40**(33): p. 4872-
344 4880.

345 26. Ndlangisa, K., et al., *Invasive Disease Caused Simultaneously by Dual Serotypes of Streptococcus*
346 *pneumoniae*. *J Clin Microbiol*, 2018. **56**(1).

347 27. Zhou, M., et al., *Serotype Distribution, Antimicrobial Susceptibility, Multilocus Sequencing Type*
348 *and Virulence of Invasive Streptococcus pneumoniae in China: A Six-Year Multicenter Study*.
349 *Front Microbiol*, 2021. **12**: p. 798750.

350 28. Ceyhan, M., et al., *Serotype distribution of Streptococcus pneumoniae in children with invasive*
351 *disease in Turkey: 2015-2018*. *Hum Vaccin Immunother*, 2020. **16**(11): p. 2773-2778.

352 29. Habibi Ghahfarokhi, S., et al., *Serotype Distribution and Antibiotic Susceptibility of Streptococcus*
353 *pneumoniae Isolates in Tehran, Iran: A Surveillance Study*. *Infect Drug Resist*, 2020. **13**: p. 333-
354 340.

355 30. Isturiz, R., et al., *Expanded Analysis of 20 Pneumococcal Serotypes Associated With*
356 *Radiographically Confirmed Community-acquired Pneumonia in Hospitalized US Adults*. Clin
357 Infect Dis, 2021. **73**(7): p. 1216-1222.

358 31. Lister, A.J.J., et al., *Serotype distribution of invasive, non-invasive and carried Streptococcus*
359 *pneumoniae in Malaysia: a meta-analysis*. Pneumonia (Nathan), 2021. **13**(1): p. 9.

360 32. Wiese, A.D., M.R. Griffin, and C.G. Grijalva, *Impact of pneumococcal conjugate vaccines on*
361 *hospitalizations for pneumonia in the United States*. Expert Rev Vaccines, 2019. **18**(4): p. 327-
362 341.

363